AJNR

Apparent Diffusion Coefficient Mapping for Sinonasal Diseases: Differentiation of Benign and Malignant Lesions

M. Sasaki, S. Eida, M. Sumi and T. Nakamura

AJNR Am J Neuroradiol 2011, 32 (6) 1100-1106
doi: https://doi.org/10.3174/ajnr.A2434
http://www.ajnr.org/content/32/6/1100

ORIGINAL RESEARCH

Apparent Diffusion Coefficient Mapping for Sinonasal Diseases: Differentiation of Benign and Malignant Lesions

M. Sasaki
S. Eida
M. Sumi
T. Nakamura

EDITOR'S CHOICES

BACKGROUND AND PURPOSE: CT and MR imaging features of benign and malignant sinonasal lesions are often nonspecific. Therefore, we evaluated the ADC-based differentiation of these lesions.

MATERIALS AND METHODS: We retrospectively assessed ADCs of 61 patients with histologically proved sinonasal tumors and tumorlike lesions: 19 benign lesions, 28 malignant tumors, and 14 inflammatory lesions. Overall ADCs and percentages of total tumor area with extremely low, low, intermediate, or high ADCs (ADC mapping) were determined by using 2 b-values (500 and 1000 s/mm^2).

RESULTS: ADCs of malignant tumors ($0.87 \pm 0.32 \times 10^{-3}$ mm^2/s) were significantly lower than those of benign ($1.35 \pm 0.29 \times 10^{-3}$ mm^2/s, $P < .0001$) and inflammatory ($1.50 \pm 0.50 \times 10^{-3}$ mm^2/s, $P = .0002$) lesions. On ADC mapping, percentages of total tumor area within malignant tumors having extremely low or low ADCs were significantly ($P < .0001$) greater than those within benign and inflammatory lesions. Cutoff points for ADC mapping (≥78% of tumor areas having extremely low or low ADCs) effectively differentiated benign or inflammatory lesions and malignant tumors with 75% sensitivity, 94% specificity, 85% accuracy, and 91% positive and 82% negative predictive values, respectively. ADCs also effectively discriminated lymphomas and SCCs from other malignant tumors.

CONCLUSIONS: ADC mapping may be an effective MR imaging tool for the differentiation of benign/inflammatory lesions from malignant tumors in the sinonasal area.

ABBREVIATIONS: ADC = apparent diffusion coefficient; CE = contrast-enhanced; FS = fat-suppressed; Hetero = heterogeneously enhancing; Homo = homogeneously enhancing; Inter = intermediate; Mixed = hyper-/iso-/hypointense signals; SCC = squamous cell carcinoma; SENSE = sensitivity encoding; SPAIR = spectral-attenuated inversion recovery; SPIR = spectral presaturation with inversion recovery; SRBCT = small round blue cell tumors; T1WI = T1-weighted imaging; T2WI = T2-weighted imaging; TIC = time-intensity curve; TSE = turbo spin-echo; UDCs = undifferentiated carcinomas

The sinonasal area is affected by benign and malignant tumors and inflammatory lesions that originate from the maxillary, ethmoid, sphenoid, and frontal sinuses and the nasal cavity. Sinonasal malignancies most commonly arise in the maxillary sinus (60%), followed by the nasal cavity (20%–30%) and sphenoid sinus (10%–15%).[1] SCCs in the maxillary sinus are the most common sinonasal malignancies; however, SRBCTs, such as neuroendocrine carcinoma, olfactory neuroblastoma, malignant melanoma, and lymphoma, may be difficult to differentiate from SCCs and even from benign and inflammatory lesions.

CT and MR imaging features of sinonasal tumors and tumorlike lesions have often been described as an expansile or infiltrative soft-tissue mass with sinus wall erosion and destruction, heterogeneous signal intensity on FS T2-weighted MR images, and irregular or homogeneous enhancement after contrast medium injection. However, the imaging features of benign and malignant sinonasal lesions are often nonspecific and overlap.[2]

Diffusion-weighted imaging has been used in the diagnosis of extracranial lesions; for example, recent studies showed that ADC measurement was useful in the differentiation of benign and malignant lesions of the lymph nodes and salivary glands.[3-6] Low ADCs indicate limited diffusion of water molecules in the tissue. Theoretically, therefore, a tumor or area within a tumor with low ADC contains a greater number of cells than one with high ADC. Consistent with this notion, lymphomas and undifferentiated cancers have lower ADCs than well-differentiated SCCs.[7] These results suggest that diffusion-weighted imaging may be applicable for the differentiation of benign and malignant sinonasal lesions.

In this study, we sought to apply ADC to differentiate benign and malignant sinonasal lesions; to further characterize heterogeneous histologic architectures of different sinonasal lesions, we also assessed the 2D distributions of ADCs (ADC mapping) on a pixel-by-pixel basis.

Materials and Methods

Subjects

Diffusion-weighted MR images were retrospectively analyzed in 61 patients (44 males and 17 females; average age, 62 ± 17 years; age range, 16–86 years) with histologically proved benign lesions, includ-

Received June 11, 2010; accepted after revision October 16.

From the Department of Radiology and Cancer Biology, Nagasaki University School of Dentistry, Nagasaki, Japan.

Please address correspondence to Takashi Nakamura, DDS, PhD, Nagasaki University School of Dentistry, 1-7-1 Sakamoto, Nagasaki 852-8588, Japan; e-mail: taku@nagasaki-u.ac.jp

Indicates article with supplemental on-line tables.

DOI 10.3174/ajnr.A2434

ing tumorlike organized hematomas, malignant tumors, and inflammatory lesions. The histology of these lesions included 19 benign lesions (7 inverted papillomas, 5 organized hematomas, 4 hemangiomas, and 3 angiofibromas); 28 malignant tumors (12 SCCs, including 5 poorly differentiated SCCs, 3 moderately differentiated SCCs, 3 well-differentiated SCCs, and 1 nonkeratinizing SCC; 6 malignant lymphomas [4 diffuse large B-cell tumors, 1 MALT lymphoma, and 1 natural killer/T-cell lymphoma]; 2 undifferentiated carcinomas; 2 metastatic renal cell carcinomas; 1 spindle-cell carcinoma; 1 melanoma; 1 olfactory neuroblastoma; 1 pleomorphic rhabdomyosarcoma; 1 adenocarcinoma; and 1 adenoid cystic carcinoma); and 14 inflammatory lesions (5 rhinosinusitis, 5 inflammatory polyps, and 4 fungus infections).

This study protocol was approved by the ethics committee of our hospital, and informed consent was obtained from all of the patients.

Diffusion-Weighted MR Imaging

Axial diffusion-weighted images (TR/TE/number of signal-intensity acquisitions = 4285/87 ms/4) were obtained by using single-shot spin-echo echo-planar imaging with an echo-planar imaging factor of 47. We used an M coil (Synergy Flex; Phillips Electronics, Best, the Netherlands) and the parallel imaging technique (SENSE; SENSE factor = 2). We also used a 200-mm FOV, 4-mm section thickness, 0.4-mm section gap, and 112 × 88 matrix size. The matrix size for reconstruction was 256 × 256. In general, when one uses b factors of >300 s/mm^2, the resultant ADC contains negligible amounts, if any, of perfusion factor.[8] Therefore, we used 2 b factors (500 and 1000 s/mm^2) to determine ADCs; actually, the obtained values indicate pure diffusion. This procedure requires additional time to be performed, but using the SENSE technique compensates for this.

Image Analysis for Diffusion-Weighted MR Imaging

Sequential gray-scale ADC map images that spanned a whole lesion, except for the upper- and lowermost sections, were saved in a DICOM format (Fig 1). Freehand regions of interest along the margins of the lesions were manually placed onto the ADC maps by using the corresponding FS T2-weighted MR images as references for placing the regions of interest. Then, average ADCs of the whole lesions were determined (overall ADCs). For ADC mapping, the gray-scale ADC maps, on which lesions were indicated by regions of interest, were converted to color ADC map images after setting the window level of gray-scale ADC map images at 1300 and the window width at 2600. As a result, disease areas having high ADCs are displayed as color areas of long wave lengths such as red and disease areas having low ADCs, as color areas of short wave lengths such as blue (Fig 1). These procedures were performed on a personal computer using OsiriX software (http://www.osirix-viewer.com). Susceptibility artifacts due to the air−soft-tissue interface or dental fillings were minimal if present, and all the MR images used in the present study were of good quality.

We classified the disease areas into 4 categories on the basis of ADC levels as previously described (Fig 1).[3] In brief, we determined the areas having extremely low ADC ($<0.6 \times 10^{-3}$ mm^2/s), low ADC (0.6×10^{-3} mm^2/s $\leq$ ADC $<1.2 \times 10^{-3}$ mm^2/s), intermediate ADC (1.2×10^{-3} mm^2/s $\leq$ ADC $<1.8 \times 10^{-3}$ mm^2/s), or high ADC ($\geq 1.8 \times 10^{-3}$ mm^2/s) relative to the total lesion on ADC maps by using the Osirix software and expressed these as percentage areas.

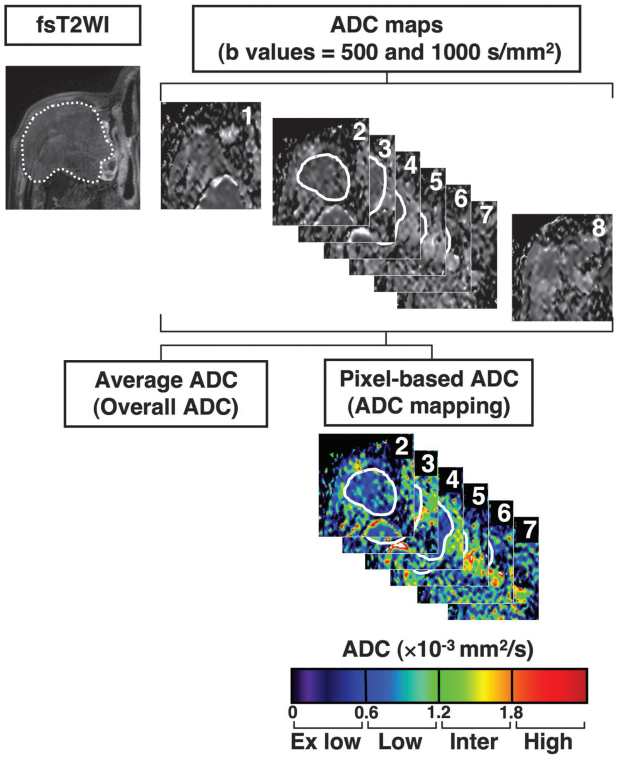

Fig 1. Overall ADC and ADC mapping. MR images are from a 77-year-old man with well-differentiated SCC. Regions of interest were manually placed on all sequential 2D ADC maps that contained tumor areas (*continuous white lines* on ADC maps 2–7), except for the upper- and lowermost sections (in this case, ADC maps 1 and 8), and onto the tumor areas of ADC maps by using the corresponding FS T2-weighted images as references for the regions of interest (*broken white line*). Then, average ADCs (overall ADCs) of the whole tumor areas were calculated. In addition, relative tumor areas with extremely low, low, intermediate, or high ADCs were separately determined and expressed as percentages of total tumor area (ADC mapping). The total time required for the ADC analyses was <10 minutes per patient. Overall ADC = 0.91×10^{-3} mm^2/s; ADC mapping of tumor areas (percentages) with extremely low/low/intermediate/high ADCs = 6 /84/9/0.

Conventional MR Imaging

We obtained axial T1-weighted (TR/TE/number of signal intensity acquisitions = 500/15 ms/2) and FS (SPIR or SPAIR) T2-weighted (TR/TE/number of signal intensity acquisitions = 4784/80 ms/2 for SPIR; 6385/80 ms/2 for SPAIR) MR images of the sinonasal lesions by using a multishot TSE sequence with a TSE factor of 3 (T1-weighted) or 15 (SPAIR). We used a 200-mm FOV, 256 × 224 scan and 512 × 512 reconstruction matrix sizes, 4-mm section thickness, and 0.4-mm section gap.

In 51 of the 61 cases, we performed contrast-enhanced T1-weighted MR imaging by using a multishot TSE sequence with a TSE factor of 7. We used a 200-mm FOV, 256 × 224 scan and matrix sizes, 5-mm section thickness, and 0.5-mm section gap. Gadopentate dimeglumine (Magnevist; Bayer HealthCare Pharmaceuticals, Wayne, New Jersey) was injected intravenously at a dose of 0.2 mL/kg of body weight and at an injection rate of 1.5 mL/s.

Consensus reading of the obtained conventional MR images was made by 3 radiologists who had experience ranging from 10 to 15 years in head and neck radiology.

Diagnostic Ability of ADC Criteria

Diagnostic ability (sensitivity, specificity, accuracy, and positive and negative predictive values) was calculated to determine compromised ADC cutoff points for the differentiation of various types of sinonasal diseases on the basis of overall ADC or pixel-based ADC (ADC map).

Conventional MR imaging findings of sinonasal tumors and tumorlike lesions

	No.	T1WI[a]		FS T2WI[b,c]			CE[d]	
		Isointense	Mixed	Isointense	Hyperintense	Mixed	Homo	Hetero
Inflammation	14	8	6	0	6	8	1	11
Benign	19	13	6	3	2	14	2	10
Malignant	28	23	5	6	0	22	8	19

[a] Lesions were categorized into those with isointense or mixed signals relative to the neighboring muscles.
[b] Lesions were categorized into those with isointense or mixed signals relative to the cerebral cortex.
[c] Differences in distributions were significant between inflammatory and benign lesions ($P = .0494$), and between inflammatory and malignant lesions ($P = .0004$), but not between benign and malignant lesions ($P = .2049$) (χ^2 test).
[d] CE MR imaging was performed in 12 inflammatory, 12 benign, and 27 malignant lesions, and the lesions were categorized as homogeneously or heterogeneously enhancing after gadolinium injection.

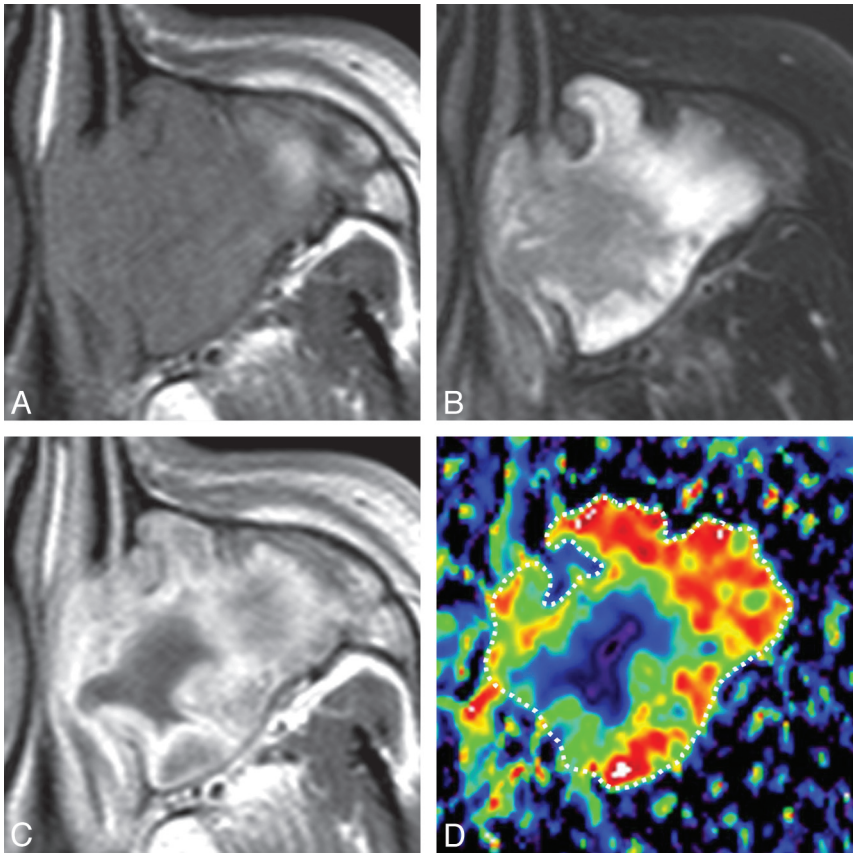

Fig 2. A 46-year-old man with rhinosinusitis. *A*, Axial T1-weighted MR image (TR/TE = 500/15 ms) shows the left maxillary sinus filled with homogeneous inflammatory tissues. *B*, Axial FS (SPAIR) T2-weighted MR image (TR/TE = 6385/80 ms) shows the left maxillary sinus filled with heterogeneous inflammatory tissues. *C*, Axial contrast-enhanced T1-weighted MR image (TR/TE = 500/15 ms) shows heterogeneously enhanced tissue in the left maxillary sinus. *D*, Axial color ADC map shows high ADC areas in the lesion periphery. Overall ADC = 2.0×10^{-3} mm^2/s. Areas with extremely low, low, intermediate, and high ADCs occupy 2%, 8%, 24%, and 66%, respectively, of the lesion.

Statistical Analysis

Differences in ADCs between different types (ie, benign, malignant, and inflammatory) of sinonasal tumors and tumorlike lesions were evaluated by the Mann-Whitney *U* test and the χ^2 test by using the statistical software StatView 4.51 (Abacus Concepts, Berkeley, California).

Results

Conventional MR Imaging

The conventional MR imaging profiles of 61 sinonasal lesions are summarized in the Table. On T2-weighted MR images, inflammatory lesions appeared with imaging features different from the benign and malignant lesions. However, the other MR imaging features (T1- and CE T1-weighted imaging) were similar among the inflammatory, benign, and malignant lesions.

Overall ADCs

Overall ADCs of malignant tumors were significantly smaller than those of benign and inflammatory lesions (Figs 2–4 and On-line Tables 1 and 2). There was no significant difference in overall ADCs between benign and inflammatory lesions.

An ADC cutoff point of 0.84×10^{-3} mm^2/s was best for differentiating benign/inflammatory lesions from malignant tumors; it provided diagnostic ability of 61% sensitivity, 94% specificity, 79% accuracy, and 90% positive and 74% negative predictive values.

ADC Mapping

ADC mapping demonstrated that disease areas with extremely low and/or low ADCs in malignant tumors were

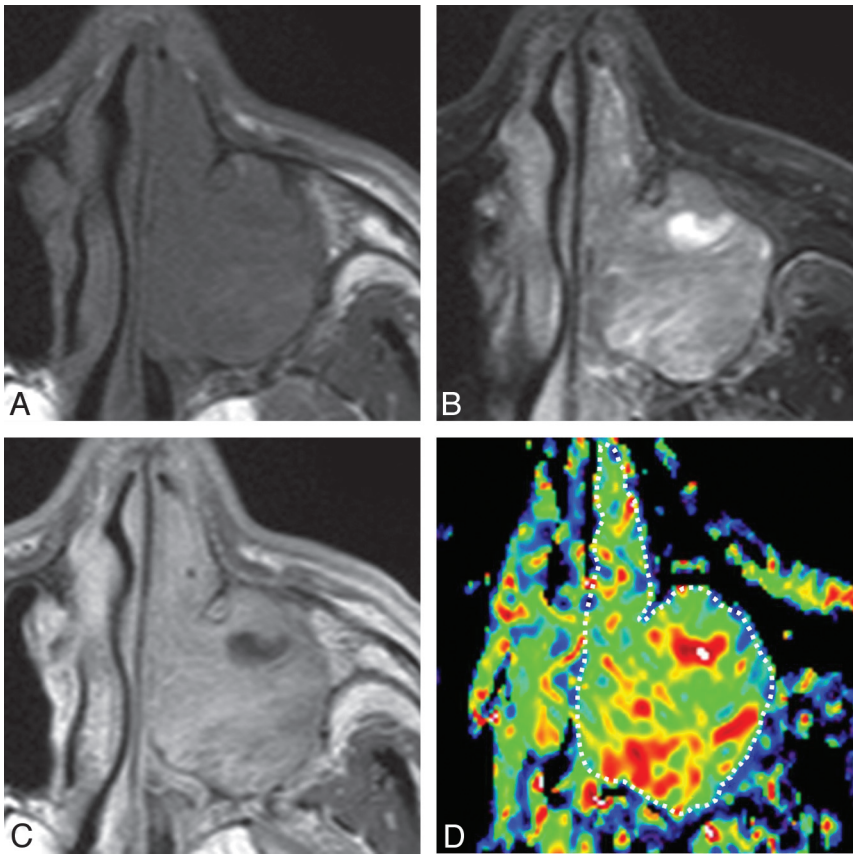

Fig 3. A 69-year-old man with inverted papilloma. *A*, Axial T1-weighted MR image (TR/TE = 500/15 ms) shows tumor with homogeneous signal intensity filling the left maxillary sinus and nasal cavity. *B*, Axial FS (SPIR) T2-weighted MR image (TR/TE = 4784 ms/80 ms) shows the tumor with heterogeneous signal intensity. *C*, Axial CE T1-weighted MR image (TR/TE = 500/15 ms) shows heterogeneously enhanced tumor. *D*, Axial color ADC map shows tumor with scattered areas of high ADCs. Overall ADC = 1.4×10^{-3} mm^2/s. Areas with extremely low, low, intermediate, and high ADCs occupy 0%, 21%, 66%, and 13%, respectively, of the tumor.

significantly greater than those in benign and inflammatory lesions (Figs 2–4 and On-line Tables 1 and 2).

A cutoff point of ≥78% of a lesion with extremely low or low ADCs positively and best discriminated the malignant tumors from the benign/inflammatory lesions with a diagnostic ability of 75% sensitivity, 94% specificity, 85% accuracy, and 91% positive and 82% negative predictive values.

ADC-Based Differentiation of Malignant Tumor Subtypes

Overall ADC and ADC mapping demonstrated that lymphomas had the smallest overall ADCs and the greatest percentages of total tumor areas with extremely low and/or low ADCs among the malignant tumors (Figs 2–4 and On-line Tables 1 and 2). Overall ADCs of SCCs (including spindle cell carcinoma and nonkeratinizing SCCs) and of undifferentiated carcinomas were significantly greater than those of the lymphomas and the percentages of total tumor area with extremely low and/or low ADCs of these malignant tumors were significantly smaller than those of the lymphomas (On-line Tables 1 and 2). However, the overall ADC parameters of the SCCs and undifferentiated carcinomas were significantly smaller than those of the other malignancies and the percentages of total tumor area with extremely low or low ADCs were greater than those of the other malignancies.

ADC-Based Differentiation of Inflammatory and Benign Lesion Subtypes

Fungus infections and organized hematomas had significantly smaller overall ADC values and greater percentages of total tumor areas with extremely low or low ADCs among the inflammatory and benign lesions (On-line Tables 1 and 2). On the other hand, fungus infections and hematomas had significantly greater overall ADCs and smaller percentages of total tumor areas with extremely low or low ADCs than the malignant lymphomas, SCCs, and undifferentiated carcinomas (On-line Tables 1 and 2).

Discussion

In this preliminary report, we evaluated ADC measurements on a lesion basis (overall ADCs) or on a pixel-by-pixel basis (ADC mapping) for the diagnosis of sinonasal tumors and tumorlike lesions. We demonstrated that overall ADC and ADC mapping effectively differentiated benign/inflammatory lesions from malignant tumors in the sinonasal area. In addition, these MR imaging techniques effectively differentiated some types of malignant tumors (lymphomas, SCCs including some SCC subtypes, and undifferentiated cancers) or benign lesions (fungus infections and organized hematomas) from the other malignant, inflammatory, or benign lesions examined. Most important, differentiation by ADC mapping pro-

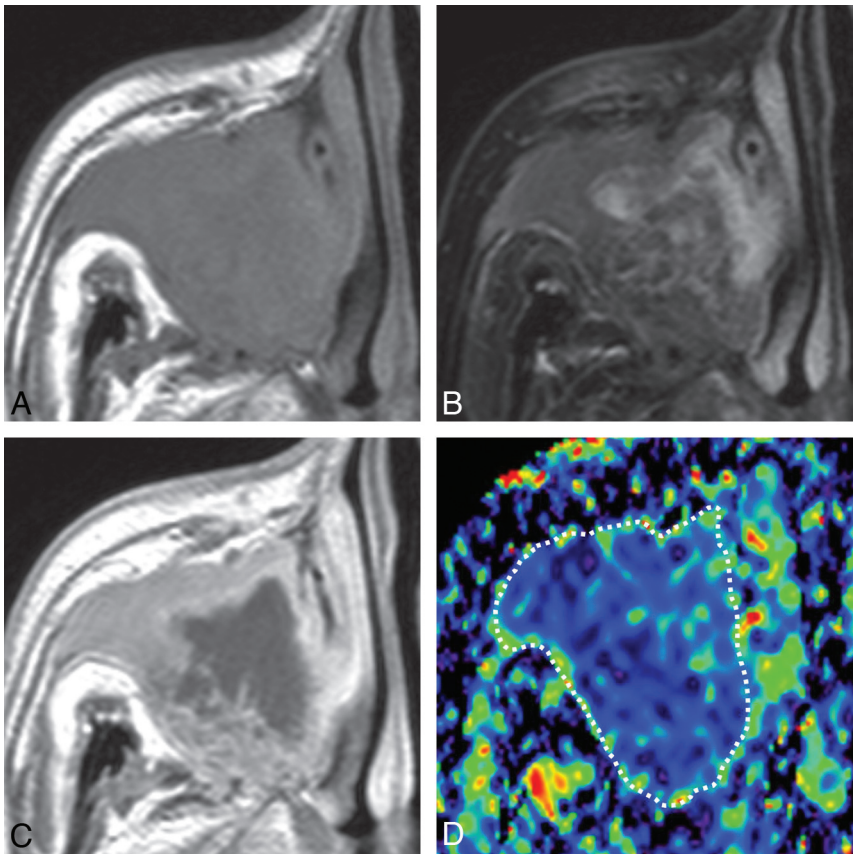

Fig 4. A 65-year-old man with SCC. *A*, Axial T1-weighted MR image (TR/TE = 500/15 ms) shows tumor with homogeneous signal intensity occupying the right maxillary sinus and extending into the surrounding bony structures. *B*, Axial FS (SPAIR) T2-weighted MR image (TR/TE = 6385/80 ms) shows tumor with heterogeneous signal intensity. *C*, Axial contrast-enhanced T1-weighted MR image (TR/TE = 500/15 ms) shows tumor with peripheral enhancement. *D*, Axial color ADC map shows tumor with a low ADC. Overall ADC = 0.8×10^{-3} mm^2/s. Areas with extremely low, low, intermediate, and high ADCs occupy 17%, 78%, 5%, and 0%, respectively, of the tumor.

vided better diagnostic ability than differentiation by overall ADC.

Because the diffusion process is dominated by its environment and the obstacles it encounters, diffusion imaging becomes a unique technique allowing us to probe structures well below the spatial resolution of the images. The diffusion-weighted signal intensity decays exponentially with respect to the b-factor of the sequence.[9] Typical b-values for clinical diffusion-weighted imaging depend on the anatomy of interest.[8,10] For organs with an intrinsically high ADC (for example, the prostate), higher b-values are needed to give a good contrast with lesions. In general, one wants to keep the b-value as low as possible because there is a signal intensity–to-noise ratio penalty when going to higher b-values. However, with the use of low b-values ($<$300 s/mm^2), the perfusion component of the tissue will hamper the pure diffusion measurement.[8,10] Therefore, many researchers have used 2 b-values (such as 500 and 1000 s/mm^2) to calculate ADCs (in this case, almost equivalent to the diffusion coefficient, *D*) of head and neck lesions.

Recent studies have demonstrated the usefulness of ADC measurement in differentiating several sets of various types of head and neck diseases; for example, compromised ADC thresholds effectively differentiated SCC metastatic nodes and nonmetastatic reactive nodes in the neck[11] and pharyngeal SCCs and extranodal lymphomas.[7] In addition, the use of manually placed small regions of interest on specified areas of a metastatic or lymphoma node can precisely predict the histologic features of cancer focus, liquefaction or coagulation necrosis, or lymphoid parenchyma. However, the ADC measurement was less effective in differentiating benign lesions from malignant tumors with more heterogeneous histologic architectures.

In a recent attempt to differentiate benign and malignant salivary gland tumors, ADC mapping based on pixel-by-pixel analysis of the whole tumor volume was found to effectively distinguish these 2 histologic entities.[3] In the present study, we found that ADC mapping was also promising in differentiating benign lesions and malignant tumors in the sinonasal area. On ADC mapping, each tumor was classified into 4 tumor areas (those with extremely low, low, intermediate, and high ADCs) as previously reported.[3] Prior studies have shown that areas with high ADCs are rare or very limited in malignant tumors.[3,12] Thus, the presence of tumor areas with high ADCs could be an important criterion in differentiating benign lesions from malignant tumors. In malignant tumors, areas with extremely low or low ADCs were found to occupy major parts of the tumor, consistent with high cellularity and, thus, the high ratio of intracellular water to extracellular water of malignant tumors. These results were consistent with the present findings that a cutoff point of $\geq$78% of tumor area having extremely low or low ADCs differentiated benign or inflammatory lesions from malignant tumors with good diagnostic reliability. Furthermore, the diagnostic ability determined on

the basis of the ADC mapping was significantly higher than that determined on the basis of overall tumor ADCs.

A previous study showed that a less than 5% tumor area having high ADCs ($\geq 1.8 \times 10^{-3}$ mm^2/s) positively indicated the malignancy of salivary gland tumors.[3] In the present study, we obtained the best differentiation of sinonasal pathology by using an ADC criterion of ≥78% area with extremely low or low ADCs; other ADC map criteria (eg, tumor area with high ADCs) were less effective for that purpose. In addition, low cutoff values for the overall tumor ADC effectively differentiated benign and malignant tumors of the head and neck in the present and previous studies.[6,11,13,14] Taken together, these results suggest that the ADC could be used for the preoperative diagnosis of malignant tumors in the head and neck.

In contrast, overall ADCs or ADC mapping failed to differentiate benign and inflammatory lesions. However, the percentages of total tumor area with extremely low and low ADCs of organized hematomas and fungus infections were significantly greater than those of the other inflammatory and benign lesions, and the percentages were significantly lower than those of malignant tumors (On-line Tables 1 and 2). Therefore, ADC mapping may be useful in differentiating organized hematomas and fungus infections from benign/malignant tumors. Histopathologically, the organized hematoma is composed of fibrous tissues surrounding an organized or old hematoma. On MR images, the lesion is often described as an expansile soft-tissue mass with sinus wall erosion, heterogeneous signal intensity with a hypointense peripheral rim on FS T2-weighted MR images, and papillary enhancement after contrast medium injection.[15] However, the imaging features are often nonspecific. In organized hematomas, organized or coagulated hematoma areas may be associated with low ADCs. The organized hematoma per se is not a cell-rich disease. Therefore, the variation in areas with extremely low and low ADCs may reflect the proportion of organized and/or coagulated areas relative to the total area.

MR imaging signals of sinonasal infectious diseases may be related to varying properties of secretions in the lesion.[16] For example, paramagnetic properties of fungus infections or hemorrhage may cause a signal-intensity void on T2-weighted images due to the paramagnetic effects of either iron or manganese production by the fungi; however, this phenomenon may also be seen in a mucocele with superimposed infection (pyocele), in which iron-loaded siderophores are present.

Effective diagnosis of sinonasal benign lesions only on the basis of conventional MR imaging may also be difficult. A convoluted cerebriform pattern is a reliable MR imaging feature of sinonasal inverted papillomas, but it is lacking in many cases (such an imaging feature was seen in 2 of the 7 present cases).[17] Signal-intensity voids are characteristic MR imaging features of angiofibromas with high vascularity,[18] but they also may be absent (seen in 2 of the 3 present cases). Finally, in the present study, there were no significant differences in overall ADCs or ADC mapping between inverted papillomas, angiofibromas, and hemangiomas (On-line Tables 1 and 2).

The present patient cohort included 11 patients with SRBCTs. This heterogeneous group of malignant neoplasms shared common histologic characteristics; comprised 20%–30% of tumors of the sinonasal region; and included lymphoma, undifferentiated carcinoma, nonkeratinizing SCC, malignant melanoma, neuroendocrine carcinoma, olfactory neuroblastoma, and rhabdomyosarcoma.[19] Although, to our knowledge, comprehensive imaging studies on this tumor entity have not yet been reported, we found that the SRBCTs displayed a wide range of overall ADCs and ADC mapping profiles (On-line Tables 1 and 2), indicating varying rates of intracellular/extracellular ratios despite their common cellular phenotypes, with relatively small-sized nuclei and scant cytoplasm.[19]

A significant flaw of this study is that the ADC mapping was not successfully correlated with the histologic features of the excised specimens; this was partly because excisional biopsy and/or other therapeutic interventions were made before the tumors were excised for histology, but mainly because all the histologic specimens needed for correlation with the ADC mapping that spanned almost all of the tumor area were, in many cases, unavailable. In this regard, previous studies have successfully correlated ADC maps with histologic findings of excised salivary gland tumors.[3,12] The authors found that among the salivary gland tumor components, lymphoid tissues had the lowest ADCs and cystic cavities had the greatest ADCs. The ADCs of growing tumor area were low but greater than those of lymphoid tissue. Increases in the amounts of fibrous connective tissue resulted in decreases in ADC levels. These results may be useful in interpreting the ADC maps of the sinonasal lesions analyzed in the present study. However, direct comparison between ADC maps and corresponding histologic features of sinonasal lesions is needed in future studies to confidently interpret ADC map profiles.

Another shortcoming of this study is that the diagnostic accuracy provided by overall ADC measurement or ADC map analysis was still insufficient for preoperative differentiation between benign lesions and malignant tumors. For example, there was a significant overlap in ADC mapping results between subtypes of inflammatory/benign lesions and malignant tumors (On-line Tables 1 and 2). In this regard, multiparametric MR imaging was reported to be effective in differentiating benign and malignant salivary gland tumors.[12,20] Therefore, a combined use of diffusion-weighted and dynamic CE MR imaging may improve the diagnostic accuracy of differentiating benign lesions from malignant tumors in the sinonasal area. To facilitate this, a recently developed MR imaging factor-analysis technique, which is also based on the pixel-by-pixel analysis of TIC patterns, would be useful[21,22]; the 2D analysis of the TIC profiles (MR imaging factor analysis) and ADC maps may enable the pixel-by-pixel evaluation of contrast enhancement kinetics and ADCs in sinonasal tumors and tumorlike lesions. The tissue ADC levels are primarily determined by cell attenuation. On the other hand, the tissue TIC patterns are largely dependent on vascular attenuation. Therefore, the combined use of ADC mapping and TIC analysis of sinonasal lesions could facilitate the understanding of the disease states, thereby significantly improving the diagnostic accuracy for the diseases.

Conclusions

We successfully applied diffusion-weighted imaging to the differentiation of benign lesions and malignant tumors in the sinonasal area. In particular, ADC mapping may facilitate the

preoperative understanding of tissue properties characteristic of malignant sinonasal tumors.

References

1. Barnes L, Everson JW, Reichart P, et al, eds. *Pathology and Genetics of Head and Neck Tumours: World Health Organization Classification of Tumours.* Lyon, France: IARC Press; 2005
2. Madani G, Beale TJ, Lund VJ. **Imaging of sinonasal tumors.** *Semin Ultrasound CT MR* 2009;30:25–38
3. Eida S, Sumi M, Sakihama N, et al. **Apparent diffusion coefficient mapping of salivary gland tumors: prediction of the benignancy and malignancy.** *AJNR Am J Neuroradiol* 2007;28:116–21
4. Sumi M, Nakamura T. **Diagnostic importance of focal defects in the apparent diffusion coefficient-based differentiation between lymphoma and squamous cell carcinoma nodes in the neck.** *Eur Radiol* 2009;19:975–81
5. Habermann CR, Arndt C, Graessner J, et al. **Diffusion-weighted echo-planar MR imaging of primary parotid gland tumor: is a prediction of different histologic subtypes possible?** *AJNR Am J Neuroradiol* 2009;30:591–96
6. Vandecaveye V, De Keyzer F, Vander Poorten V, et al. **Head and neck squamous cell carcinoma: value of diffusion-weighted MR imaging for nodal staging.** *Radiology* 2009;251:134–46
7. Sumi M, Ichikawa Y, Nakamura T. **Diagnostic ability of apparent diffusion coefficients for lymphomas and carcinomas in the pharynx.** *Eur Radiol* 2007;17:2631–37
8. Thoeny HC, De Keyzer F, Boesch C, et al. **Diffusion-weighted imaging of the parotid gland: influence of the choice of b-values on the apparent diffusion coefficient value.** *J Magn Reson Imaging* 2004;20:786–90
9. Le Bihan D. **The 'wet mind': water and functional neuroimaging.** *Phys Med Biol* 2007;52:R57–90. Epub 2007 Mar 9
10. Padhani AR, Liu G, Koh DM, et al. **Diffusion-weighted magnetic resonance imaging as a cancer biomarker: consensus and recommendations.** *Neoplasia* 2009;11:102–25
11. Sumi M, Sakihama N, Sumi T, et al. **Discrimination of metastatic cervical lymph nodes with diffusion-weighted MR imaging in patients with head and neck cancer.** *AJNR Am J Neuroradiol* 2003;24:1627–34
12. Eida S, Sumi M, Nakamura T. **Multiparametric magnetic resonance imaging for the differentiation between benign and malignant salivary gland tumors.** *J Magn Reson Imaging* 2010;31:673–79
13. Srinivasan A, Dvorak R, Perni K, et al. **Differentiation of benign and malignant pathology in the head and neck using 3T apparent diffusion coefficient values: early experience.** *AJNR Am J Neuroradiol* 2008;29:40–44
14. Abdel Razek AA, Gaballa G, Elhawarey G, et al. **Characterization of pediatric head and neck masses with diffusion-weighted MR imaging.** *Eur Radiol* 2009;19:201–08
15. Kim EY, Kim HJ, Chung SK, et al. **Sinonasal organized hematoma: CT and MR imaging findings.** *AJNR Am J Neuroradiol* 2008;29:1204–08
16. Eggesbø HB. **Radiological imaging of inflammatory lesions in the nasal cavity and paranasal sinuses.** *Eur Radiol* 2006;16:872–88
17. Jeon TY, Kim HJ, Chung SK, et al. **Sinonasal inverted papilloma: value of convoluted cerebriform pattern on MR imaging.** *AJNR Am J Neuroradiol* 2008;29:1556–60
18. Lloyd G, Howard D, Lund VJ, et al. **Imaging of juvenile angiofibroma.** *J Laryngol Otol* 2000;114:727–30
19. Bridge JA, Bowen JM, Smith RB. **The small round blue cell tumors of the sinonasal area.** *Head Neck Pathol* 2010;4:84–93
20. Yabuuchi H, Matsuo Y, Kamitani T, et al. **Parotid gland tumors: can addition of diffusion-weighted MR imaging to dynamic contrast-enhanced MR imaging improve diagnostic accuracy in characterization?** *Radiology* 2008;249:909–16
21. Zagdaniski AM, Sigal R, Bosq J, et al. **Factor analysis of medical image sequences in MR of head and neck tumors.** *AJNR Am J Neuroradiol* 1994;15:1359–68
22. Eida S, Ohki M, Sumi M, et al. **MR factor analysis: improved technology for the assessment of 2D dynamic structures of benign and malignant salivary gland tumors.** *J Magn Reson Imaging* 2008;27:1256–62